

This material is posted here with permission of the IEEE. Such permission of the IEEE does not in any way imply IEEE endorsement of any of Helsinki University of Technology's products or services. Internal or personal use of this material is permitted. However, permission to reprint/republish this material for advertising or promotional purposes or for creating new collective works for resale or redistribution must be obtained from the IEEE by writing to [pubs-permissions@ieee.org](mailto:pubs-permissions@ieee.org).

By choosing to view this document, you agree to all provisions of the copyright laws protecting it.

# Comparison of MIMO Antenna Configurations in Picocell and Microcell Environments

Kati Sulonen, Pasi Suvikunnas, Lasse Vuokko, Jarmo Kivinen, and Pertti Vainikainen, *Member, IEEE*

**Abstract**—This paper presents the results achieved with a dual-polarized multiple-input multiple-output (MIMO) measurement system in the 2 GHz range. Results from continuous measurement routes were used in evaluating and comparing different MIMO antenna configurations. Different pattern and polarization diversity possibilities were studied using two methods: elements were selected from the antenna arrays used in measurements, and as another option, in the mobile station the incident waves were estimated and used in different dipole antenna arrays. The capacity limit seems to be higher in an indoor picocell than in an outdoor microcell environment. At the mobile station, directive elements result in 35% higher average capacities than those of the omnidirectional elements; however, the capacity of the directive elements also depends on the azimuth direction of arrival of the incident field. Dual-polarized antenna configurations have approximately 14% higher capacities than copolarized configurations. Increasing the number of mobile antenna elements increases the capacity in those environments where the angular spread of the incident field is large. Increasing the distance between elements at the fixed station increases the capacity—especially in microcells where signals arrive from specific directions.

**Index Terms**—Antenna configuration, base station antenna, mobile terminal antenna, multiple-input multiple-output (MIMO) measurements.

## I. INTRODUCTION

**S**INGLE-INPUT single-output (SISO) systems with one antenna at each end of the link have traditionally been used in mobile radio communications. By adding more antennas to one end of the link, the capacity can be increased as a result of diversity [1] and antenna array gain. In multimedia applications, for example, even more capacity is needed and, therefore, the idea of adding several antennas at both ends of the link has been considered. Multiple-input multiple-output (MIMO) systems can provide radio channels capable of transferring parallel information within the same bandwidth and increase the attainable capacity [2], [3].

The capacity limit for an error-free bit rate for a radio link can be calculated using the well-known Shannon capacity theorem extended to multielement systems [4]. In [4], indepen-

dent and identically distributed (i.i.d.) Rayleigh-fading channels have been assumed, although in reality radio channels are not uncorrelated and several mechanisms affect the attainable capacity—such as the number of antennas, the type of antenna element and spacing, and the propagation environment. The capacity of MIMO antennas generally decreases with a narrowing of the angle spread [3], [5] due to the increased correlation between the antenna elements. According to [6], the degradation in capacity caused by the fading correlation of up to 0.5 is small for a MIMO system of four transmitting and receiving antenna elements. Regardless of the rich scattering environment, the existence of separate channels is not guaranteed due to the possible “keyhole” effect [7]. In the open-loop systems where the transmitter does not know the propagation channel, the power is distributed equally to all transmitting (Tx) elements [2]. In closed-loop systems where the channel is known, the water-filling scheme [8] has been suggested whereby complex weights are set to Tx elements in order to maximize capacity.

Simulations [2], [3], [5] are not adequate for studying MIMO systems due to the limited knowledge of channel parameters and measurements are, therefore, needed. The directions of departure and arrival have been studied experimentally at 5.2 GHz in [9] and [10]. The effect of the antenna element spacing on capacity caused by changes in correlation can be significant at the base station [3], [11]. In designing MIMO systems correlation has to be taken into account, since in small mobile terminals such as portable computers, wireless personal digital assistants, and mobile phones, the antenna elements have to be closely spaced. Antenna configurations consisting of either omnidirectional or directive elements can be used in MIMO systems [12]. Polarization diversity has been suggested as an attractive solution for obtaining uncorrelated antenna elements [13]. In [6] and [14], three fixed station MIMO antenna configurations with different polarization and spatial properties were also studied using different antenna configurations on a portable computer at the mobile station.

This paper is based on the approach taken at the Helsinki University of Technology, where a broadband measurement system of up to eight dual-polarized antennas at the transmitter and up to 32 dual-polarized antennas at the receiver, has been developed for MIMO measurements at 2.15 GHz [15]. The results obtained with this system enable many important and unique evaluation studies of different mobile (MS) and fixed station (FS) antenna configurations.

- The large number of measurement channels enables the study of different antenna configurations by simply selecting antenna elements from the arrays. The extraction of incident waves and their corresponding properties

Manuscript received January 5, 2002; revised May 12, 2002. This work was partially funded by Academy of Finland, System Technology For Future Wireless Telecommunication project of TEKES, Nokia Research Center, Omnitele and Sonera, and Graduate School in Electronics, Telecommunications, and Automation. This work was supported in part by the HPY foundation, Nokia Foundation, Foundation for Commercial and Technical Sciences, Foundation of Technology (Finland), and Finnish Society of Electronics Engineers.

The authors are with the Helsinki University of Technology, Radio Laboratory, FIN-02015 HUT, Finland (e-mail: kati.sulonen@hut.fi; pasi.suvikunnas@hut.fi; lasse.vuokko@hut.fi; jarmo.kivinen@hut.fi; pertti.vainikainen@hut.fi).

Digital Object Identifier 10.1109/JSAC.2003.810297

enable the comparison of antennas with arbitrary radiation patterns.

- A complete polarization state is always available; this is necessary since orthogonal polarizations are potential parallel information carriers. Dual-polarized antennas are, moreover, compact and thus easily integrated in the mobile devices.
- At the MS, the spherical array gives a complete angular coverage, thus enabling comparisons between directive and omnidirectional radiation patterns of MIMO antennas.
- Long continuous measurements enable large scale effects to be included in the antenna evaluation. From the point of view of planning the radio network, the average MIMO performance is not sufficient and the distribution of the capacity must also be known.
- A complete analysis of properties such as direction of arrival (or departure), polarization and delay distribution of incident waves can be performed for the measured routes. This information can be used for finding propagation based explanations for the performance of the antenna configurations.

In this paper, measurements are used as the experimental basis for the validation of MIMO antenna configurations. The environments were selected to represent both the expected typical-usage environments of MIMO systems and two different scattering environments. The goal is to provide new systematic information to support the optimization of realistic FS and MS antennas. Both directive and omnidirectional antenna elements were studied at the MS. The configurations range from a single dual-polarized antenna that is possible in a mobile handset to eight-channel antenna configurations applicable in portable computer-type devices. At the FS, different linear antenna arrays were studied to clarify the significance of the size of the array on MIMO performance.

The measurement system is described in Section II together with the methods used in analyzing the data in Section III. Section IV presents the capacity results for different antenna configurations and directions of arrival for incident field at the MS. The conclusions are drawn in Section V.

## II. MIMO MEASUREMENTS

### A. Measurement System

A horizontal zigzag antenna array and a linear antenna array of eight directive and dual-polarized antenna elements (Fig. 1) were used at the FS in both indoor and outdoor environments, respectively. The spherical antenna array of 32 directive and dual-polarized antenna elements located on the sphere was also used at the receiving (Rx) MS [16]. One dual-polarized element consists of two orthogonally polarized channels. Antenna arrays at the FS and MS were connected to the transmitter and to the receiving wideband radio channel sounder [17], respectively, with high-speed RF switches. The high-speed switches and a data collection unit capable of storing a  $2 * 20$  Mbyte/s stream of complex data to hard disks enable continuous measurements along approximately 300-m routes. Due to the power handling capability of the Tx switch,

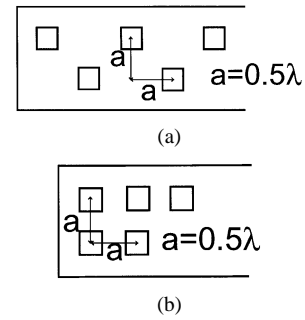


Fig. 1. (a) Zigzag array. (b) Linear array.

the transmitted power had to be limited to +26 dBm, thus reducing the maximum measurement distance and limiting the use of the system to mainly picocells and microcells. A pseudonoise code with 30-MHz chip frequency was used, corresponding to a delay resolution of 33 ns. The velocity of movement was approximately 0.4 m/s, meaning in practical terms that a trolley carrying the MS moved 3.5 mm during the measurement of one complex channel matrix, causing an error of a fraction of a degree in the angular domain analysis.

In the measurements, a vertically polarized omnidirectional discone antenna [18] connected to one channel at the MS was used for adjusting the automatic gain control of the radio channel sounder and also as a reference antenna in the analysis. The discone was located 0.20 m lower and 0.37 m to the rear left with respect to the center of the spherical antenna array.

In this paper, we use the terms vertical polarization (VP) and horizontal polarization (HP) meaning in practice  $\theta$  and  $\phi$  polarizations in standard coordinates for the spherical antenna array, respectively [16]. The  $z$  axis ( $\theta = 0^\circ$ ) points upwards, the  $x$  axis ( $\phi = 0^\circ$ ) points to the moving direction of the trolley, and the  $\phi$  angles increase in a counterclockwise direction.

### B. Measurement Environments

Two potential MIMO environments, indoor picocell and outdoor microcell, were included in the measurements. In downtown Helsinki, the FS was located below rooftop level at a height of 13 m, pointing along the street; the MS was carried by a trolley which moved along the street and across an intersection [“ $R_{out}$ ” in Fig. 2(a)]. Two different FS locations were used inside a large office building: FS1 was at a height of 5.2 m and FS2 at a height of 3.8 m [see Fig. 2(b)]. The first measurement was performed along the route “B” on the second floor, where the receiver was moved from a hall into a room using FS1. The second route “A” beginning in an open hall and ending in a corridor was measured on the first floor using FS2. The direction of motion of the MS and the broadside directions of the FS antenna arrays are marked in figures by arrowheads.

## III. DATA ANALYSIS

The capacity of the MIMO configurations studied was calculated following Shannon’s capacity theorem [2], [3], [5]. This theoretical capacity limit is useful for antenna comparisons although it cannot be reached in practice. In this paper, two different analysis methods—element selection and simulated

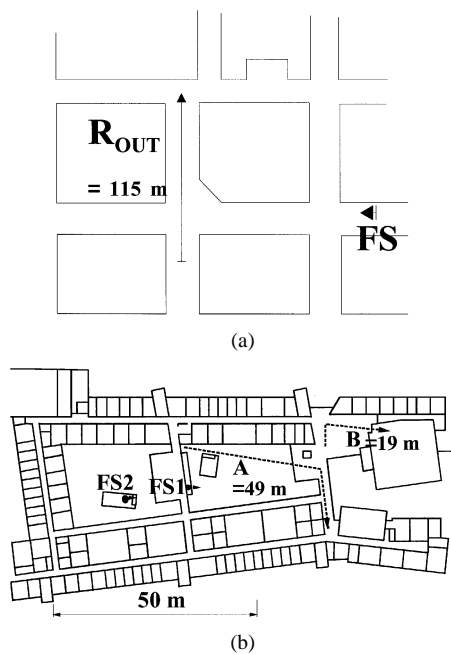


Fig. 2. Maps of measurement routes and transmitter locations. (a) Outdoor microcell environment. (b) Indoor to indoor environment.

dipole antenna configurations—have been investigated to study the difference between SISO capacity and MIMO capacity of various antenna configurations.

The complex channel matrix was normalized by removing the average path loss from the matrix, which has been a procedure used by many researchers, and first introduced in [4]. Here, the channel gain used in normalization was averaged over a sliding window of about 1 m, corresponding to  $7\lambda$ , in order to mitigate the effects of slow fading (see also Section IV-A). In real networks, a similar situation occurs as the power control tries to keep the received signal-to-noise ratio (SNR) constant. Failure to do this would clearly increase the capacity due to the increased SNR—for example in a line-of-sight connection. The normalized instantaneous channel correlation matrix was calculated according to

$$\bar{R}_{\text{norm}} = \frac{\overline{\mathbf{H}^H \mathbf{H}}}{\frac{1}{n_t n_r} E \left\{ \sum_{t=1}^{n_t} \sum_{r=1}^{n_r} H_{r,t}^* H_{r,t} \right\}} \quad (1)$$

where  $(\cdot)^H$  is complex conjugate transpose,  $(\cdot)^*$  is complex conjugate, and  $E\{\cdot\}$  is expectation operator over the sliding window.  $n_t$  and  $n_r$  are the numbers of transmitting and receiving antenna elements, respectively.  $\bar{\mathbf{H}}$  is a narrowband complex channel matrix obtained from impulse responses by at first removing noise and then using coherent summing in the delay domain.

#### A. Element Selection

At the MS, the sizes of a portable computer and a mobile phone restrict the number of antenna elements selected from the receiving (MS) antenna array by up to one in the mobile phone sized device and by as many as to four in the portable computer; for this reason, configurations of one and four elements (see Fig. 3) have been analyzed as realistic antenna configurations. At the FS the configurations from one to seven elements have been selected.

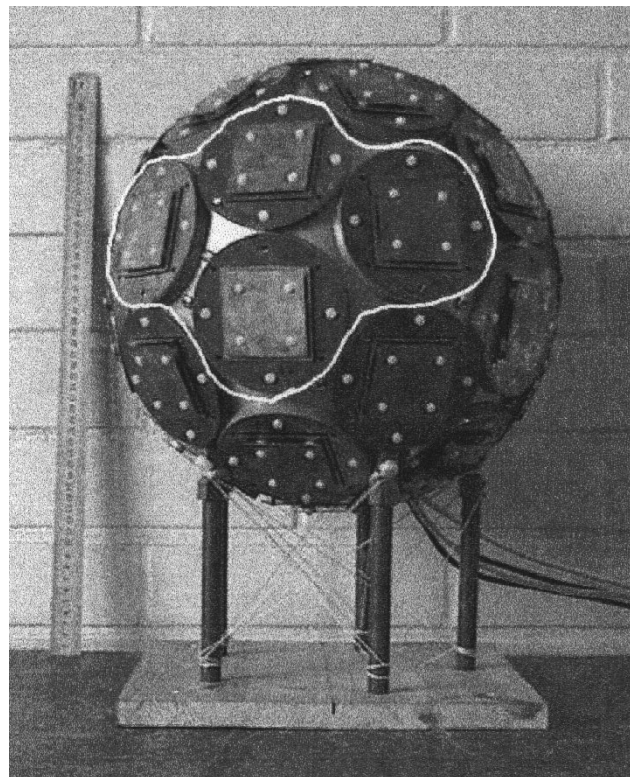


Fig. 3. One four-element configuration selected from the spherical antenna array.

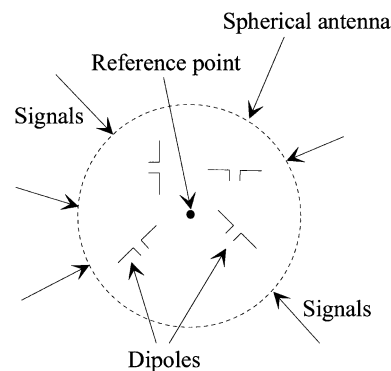


Fig. 4. Dipoles and the spherical antenna array.

The discone antenna was used as the reference antenna since the directive patch antennas toward the five different azimuth orientations on the surface of the spherical array do not receive the same average power. The average channel gain used in normalization was calculated over the connections between VP transmitting elements and the receiving discone using (1). In capacity calculations, a SNR ( $\rho$ ) of 10 dB was used for the discone.

#### B. Simulated Antenna Configurations

In the second method, the incident waves have been estimated at the MS and used with different dipole antenna arrays as illustrated in Fig. 4. With this method, arbitrary dipole configurations can be studied, enabling the study of real mobile terminal antenna configurations in the future. The configurations studied and presented in Fig. 5 consist of four dipole

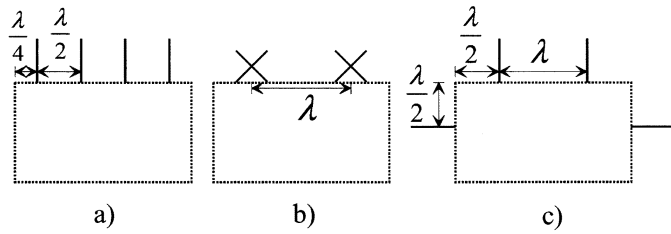


Fig. 5. Simulated antenna configurations. (a) Four vertical half-wavelength dipoles (referred as “4 ver”). (b) Two cross dipoles (referred as “2 cross”). (c) Two horizontal and two vertical dipoles (referred as “2 ver, 2 hor”).

antennas located as if they were attached to a portable computer. In this method, received field components are first solved from the spherical antenna array measurement data using the method described in [16]. Second, signal phases are calculated at the centre of the spherical antenna array used as a reference point and then at the location of each dipole element. The resolved field components can be considered as plane waves because of far field assumption. Finally, the theoretical radiation pattern of the dipole and the solved incident waves are used for calculating the received signals at each dipole [19]. Mutual coupling is ignored. In simulations, the direction of motion of the dipole group was perpendicular to the body to which the dipoles were attached. In this method, all dipole arrays receive the same average power, and normalization was performed using (1) for the selected VP transmitting elements and the VP dipole configuration in Fig. 5(a). In capacity calculations a SNR was 10 dB.

### C. Capacity Calculations

The capacity of different MIMO antenna configurations and the capacity of the discone has been calculated using the normalized instantaneous channel correlation matrix. Shannon capacity is of the form [4]

$$C = \log_2 \left[ \det \left( I + \frac{\rho}{n_t} \bar{R}_{\text{norm}} \right) \right] \quad [\text{bit/s/Hz}] \quad (2)$$

where  $\rho$  is SNR and  $I$  is the identity matrix. Only equal power allocation is studied. The number of linearly independent channels is related to the rank of the correlation matrix (number of significant eigenvalues). In the worst case—called a keyhole [7]—only one significant eigenvalue exists, whereas to achieve the maximum capacity all eigenvalues should be equal.

Thermal noise, which is normally and i.i.d., adds to the signal in the measurement process. The noise and other equipment nonidealities could influence on the accuracy of  $\bar{H}$  and thereby  $C$ . The noise contribution in  $\bar{H}$  is described by SNR in the measurement,  $\text{SNR}_m$ , and the noise influence on  $C$  can be analyzed according to [20] and [21]. The low values of  $\text{SNR}_m$  would introduce erroneous eigenvalues in  $\bar{R}_{\text{norm}}$ , resulting in erroneously high values of  $C$ , especially in a case of reflectionless far field free space propagation [20], or in a “keyhole” case.

In our off-line data processing procedure, the recorded wideband signals from different channels are first convolved with a matched filter [17] resulting in a matrix of complex impulse responses. The noise floor of each impulse response is estimated, and a detection threshold level is set 13 dB above the noise floor. The noise floor also includes certain other system nonidealities

TABLE I  
RATIO OF TRPs AT DIFFERENT TX POLARIZATIONS  
AND XPR FOR THE MEASURED ROUTES

Route	R_TRP [dB]	Tx polarization	XPR [dB]
‘Rout’	1.5	VP	12.7
		HP	10.5
‘A’	-0.4	VP	10.0
		HP	8.8
‘B’	-0.7	VP	10.0
		HP	10.9

[17].  $\text{SNR}_m$  of each element of  $\bar{H}$  can be estimated as the ratio of the mean power of the detected impulse response components and the noise floor. Thus, estimated mean  $\text{SNR}_m$  of  $\bar{H}$  is generally about 30 dB. The worst case is the NLOS in microcell, where the mean  $\text{SNR}_m$  starts to decrease due to increase of pathloss so that in the most distant point it is 22 dB. So, the influence of noise on  $C$  in the  $4 \times 8$  matrix is less than 1 bit/s/Hz in the worst measurement location ( $\text{SNR}_m = 22$  dB,  $\rho = 10$  dB) presented in this paper. Obviously, in most of the presented cases the noise influence on the capacity is smaller than that.

### D. Direction of Arrival (DoA) Analysis

The DoA analysis [16], [22] was performed to study the correlation between the measured maximal capacity and the environmental properties. In theory, all Tx signals can act as parallel MIMO subchannels, unless they are influenced by the keyhole effect or are too close to each other and cannot, therefore, be separated by the antenna arrays.

The DoA analysis was accomplished with beamforming, described in [16]. The DoA is calculated for one Tx antenna element only since the physical propagation paths are basically same for all the closely placed elements at the FS. To study the effect of the polarization of the transmitted signals, the analysis was made for both VP and HP by choosing different feeds from one FS antenna element. The Rx power was averaged over two wavelengths.

The cross-polarization power ratios (XPR) for the measured routes are presented in Table I. Here, XPR is defined as the ratio of total Rx power in the Tx polarization (VP or HP) to total Rx power in the orthogonal polarization. The ratio of total received power using at first only VP and then only HP in transmission (R\_TRP) is also presented in Table I. Because of the rather short measurement distances, coupling from one polarization to another is insignificant and the XPR values are high. DoA analysis provided almost identical results for both polarizations due to the identical propagation mechanisms. Accordingly, the DoAs are presented for only the VP Tx element in Fig. 6.

## IV. CAPACITY RESULTS

The effect of the different antenna configurations on the capacity of a MIMO system was studied by selecting elements from the linear antenna arrays at the FS and the spherical antenna array at the MS (cases 1–3). At the MS, artificial configurations with incident field-based analysis were also used (case 4). The cumulative distribution functions of capacities calculated using (1) and (2) are presented in Figs. 7–11. A SISO

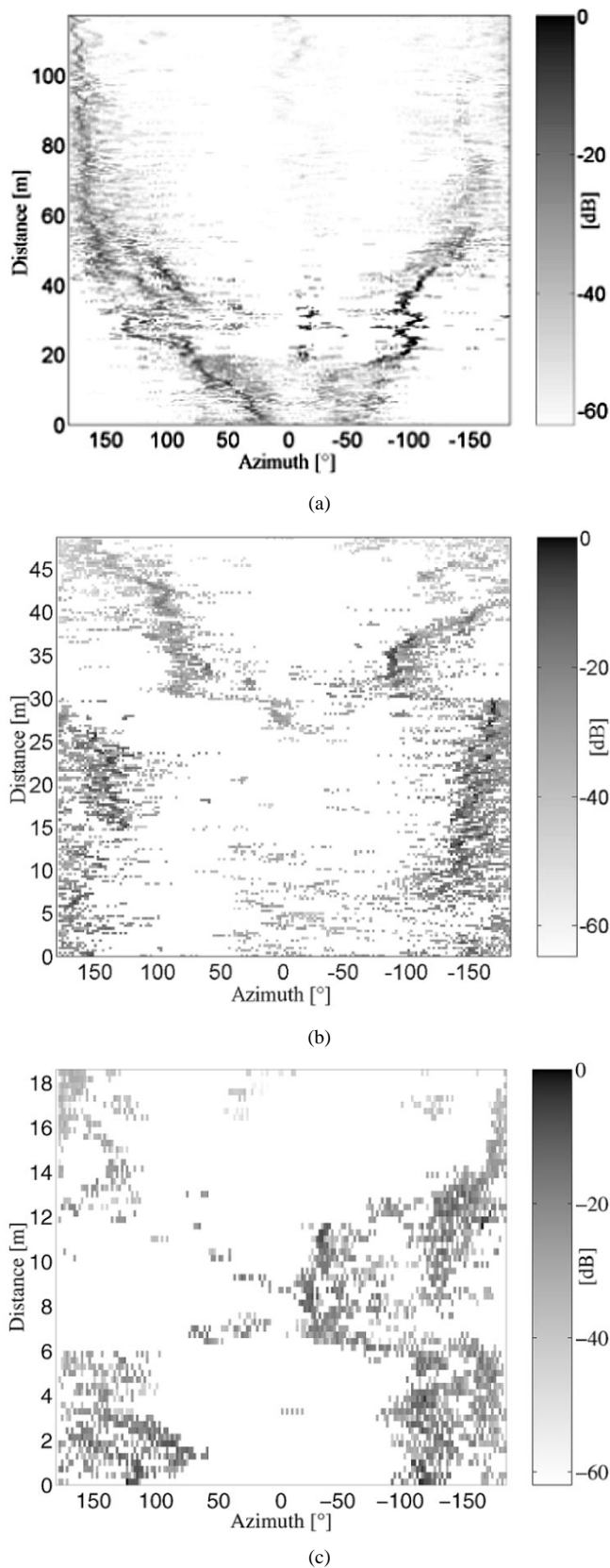


Fig. 6. Azimuth DoAs along measurement routes. (a) Route "R<sub>out</sub>." (b) Route "A" using FS2. (c) Route "B" using FS1.

capacity was calculated for the discone and one vertically polarized FS antenna element, in the cases of element selection, as

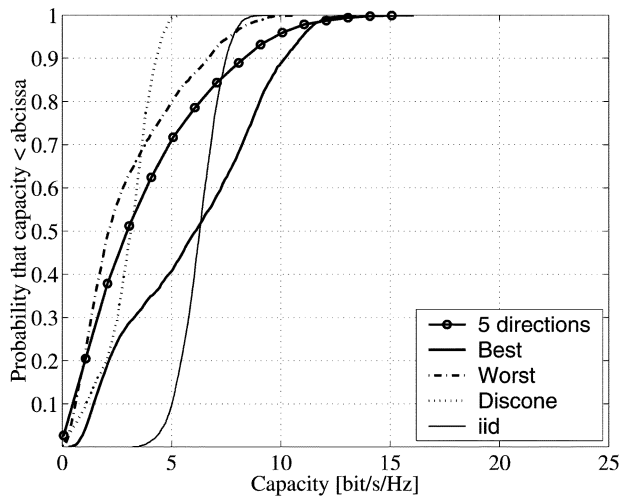
a reference for the MIMO capacity. The following is a presentation of cases 1 to 4:

- Case 1) The effects caused by the varying azimuth orientation of mobile terminal antennas with respect to the FS were studied by selecting one dual-polarized antenna element of the spherical antenna array. Such an antenna is suitable for mobile phone sized equipment. The cdfs of the capacity results were calculated by combining the results over five equally spaced azimuth orientations of the element. The capacities of the "best" and the "worst" azimuth orientations along the whole route and the reference discone antenna were also included in the analysis. At the FS two adjacent elements were used, resulting in  $4 \times 2$  MIMO configurations.
- Case 2) Effects of using either VP or HP were studied by selecting copolarized feeds of four antennas at the MS (see Fig. 3). In addition, cross-polarized channels were studied by again selecting the same four elements at the MS, but two HP and two VP feeds. At the FS two dual-polarized elements were used in case 2, resulting in a  $4 \times 4$  MIMO configuration. Five groups were analyzed as in case 1.
- Case 3) The effect of interelement spacing on capacity was studied by gradually increasing the distance between elements at the FS. At the MS four elements were used (Fig. 3) resulting in a  $4 \times 8$  MIMO configuration. Five groups were analyzed as in case 1.
- Case 4) Three different MS antenna configurations were compared in the incident field-based dipole analysis in the indoor environment. The antenna configurations were assumed to be suitable for portable computers, as illustrated in Fig. 5. The unidealities caused by the computer chassis and mutual coupling were ignored. Two dual-polarized elements were selected from the transmitting FS antenna array resulting in a  $4 \times 4$  MIMO configuration.

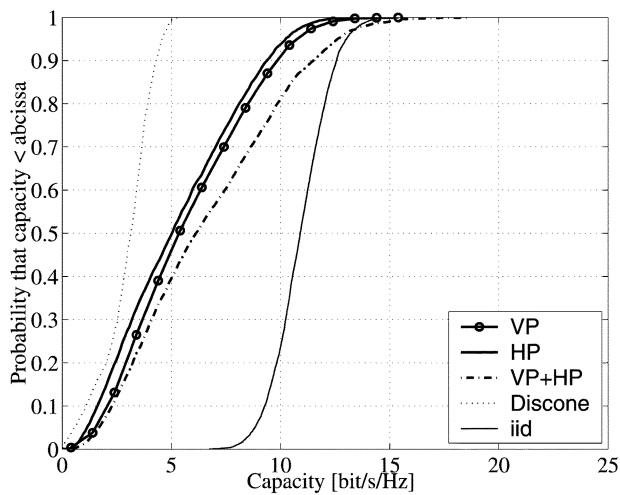
In all cases, the capacity of i.i.d. Rayleigh channels of similar size to the studied MIMO configurations was also calculated, using isotropic elements. The i.i.d. capacities have been included in the capacity figures of this paper, although they are not directly comparable with our results, as in our studies the SNR of the directive elements varied as a result of the normalization to the discone. Thus, the achieved capacities are sometimes higher than those of the i.i.d. channel.

#### A. Outdoor Environment

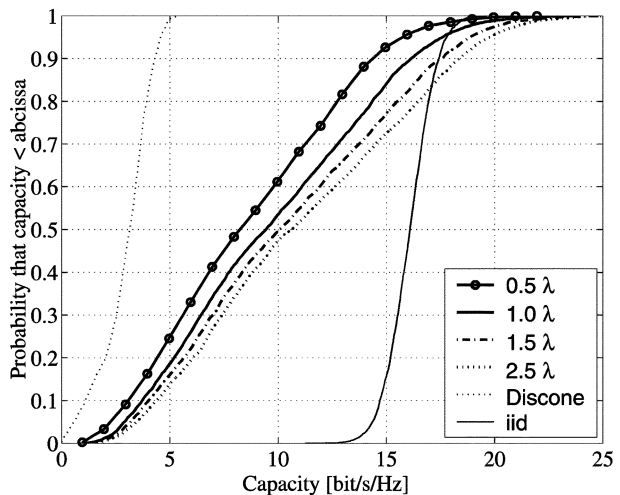
In downtown Helsinki, the transmitter was located at a height of 13 m and the receiving spherical antenna array was moved along the route "R<sub>out</sub>" (Fig. 2). The capacity between the "worst" and the "best" cases varies (Fig. 7, case 1) due to both LOS and NLOS channel connections—the mean difference being 4 bit/s/Hz. The bad azimuth orientation of the directive elements, with respect to incoming signals, reduces the capacity when compared with that of the omnidirectional discone. Considering for example, a mobile phone held to the ear, even though it may not be a typical position for the use



(a)



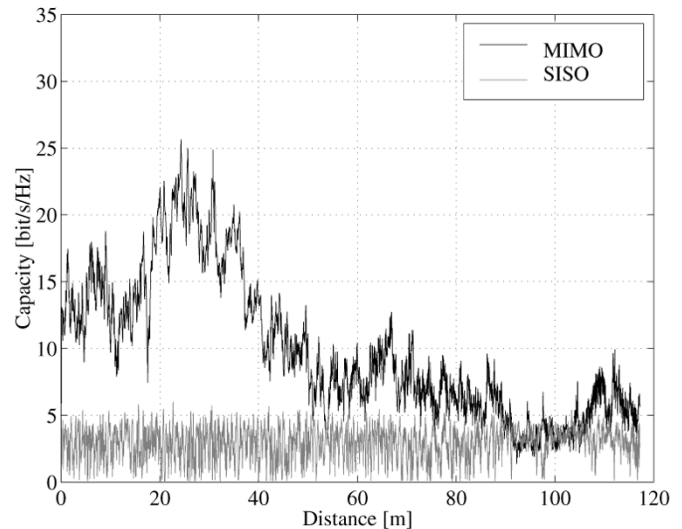
(b)



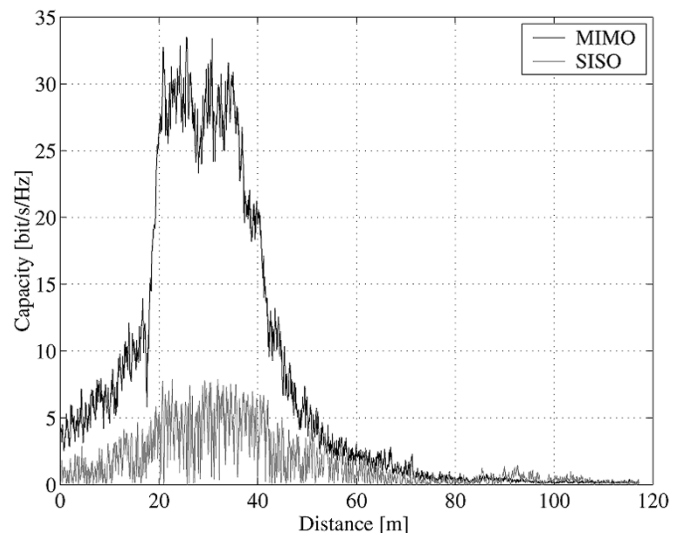
(c)

Fig. 7. Capacity results from the outdoor microcell environment. (a) Case 1, the effect of azimuth orientation,  $n_T = 4$ ,  $n_R = 2$ . (b) Case 2, the effect of polarization,  $n_T = 4$ ,  $n_R = 4$ . (c) Case 3, the effect of Tx element spacing,  $n_T = 4$ ,  $n_R = 8$ .

of MIMO equipment, the capacity can vary remarkably as a function of orientation.



(a)



(b)

Fig. 8. Comparison of two normalization methods using  $4 \times 8$  MIMO configuration with right pointing elements on the route “ $R_{out}$ .” (a) Normalized over 1 m. (b) Normalized over the route.

The capacity of the cross-polarized channels is better than that of the single polarization (case 2), possibly due to the increased effective gain of the antenna array in the environment and better matching of polarization. The effect on capacity of using either VP or HP at MS is small if orthogonal polarizations are used at the FS. Compared with the discone, four channels with two orthogonal polarizations increases the average capacity 5 bits/s/Hz (case 2). The number of channels remains at the FS but increases at the MS from four, in case 2, to eight in case 3, which is seen as a capacity improvement of 3 bit/s/Hz. Increasing the spacing of the FS elements from  $0.5\lambda$  to  $2.5\lambda$  has a clear effect on capacity—the largest increase being from  $0.5\lambda$  to  $1\lambda$  (case 3). For one Tx element the DoAs (normalized to maximum value along the route) at the MS are presented in Fig. 6(a), where the signals arrive clearly from the direction of the Tx and along the street. In an urban street, signals generally arrive from specific directions, as was also shown in [22]. A sufficiently large distance between the Tx elements increases

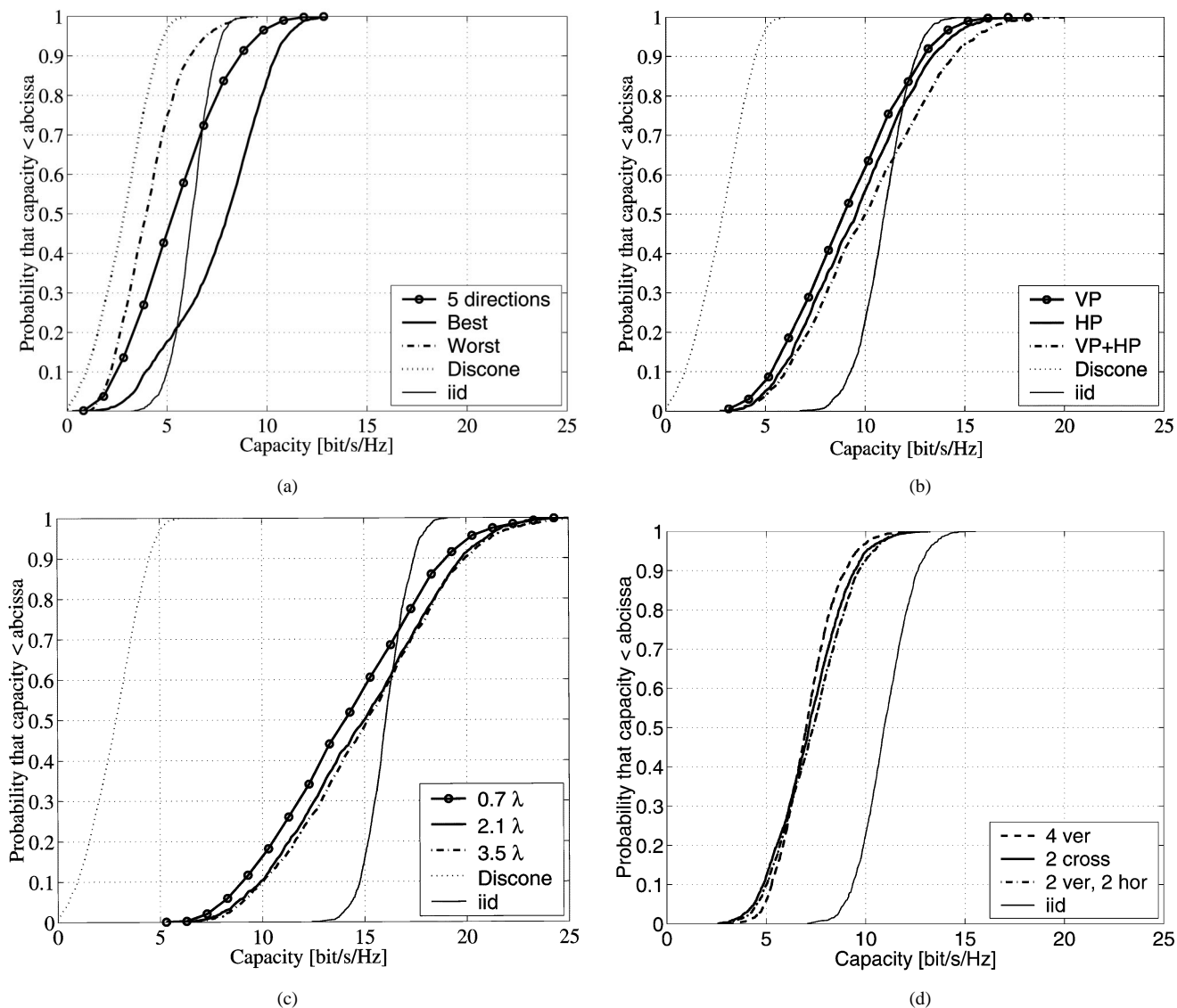


Fig. 9. Capacity results in the indoor environment FS2 “A.” (a) Case 1, the effect of azimuth orientation,  $n_T = 4$ ,  $n_R = 2$ . (b) Case 2, the effect of polarization,  $n_T = 4$ ,  $n_R = 4$ . (c) Case 3, the effect of Tx element spacing,  $n_T = 4$ ,  $n_R = 8$ . (d) Case 4, the dipole study,  $n_T = 4$ ,  $n_R = 4$ .

the variety of propagation paths and, consequently, the MIMO capacity.

The capacity of a  $4 \times 8$  MIMO configuration consisting of two Tx elements and four Rx elements in the direction of  $\phi = 270$  (the direction of Tx at the crossroads) is presented in Fig. 8. Two different normalization methods have been considered: in Fig. 8(a) the normalization is over a 1 m sliding window, whereas in Fig. 8(b), the normalization is over the whole measurement route with average SNR of 10 dB for the discone. The sliding-window normalization was selected since the latter method clearly shows the changes in SNR in the result. In both normalization methods, the capacity decreases after a distance of 50 m because the directive elements are toward a wall and no signals can be separated from noise.

### B. Indoor Route “A” FS Location 2

Route “A” begins in an open hall inside the office building and ends in a corridor, which can clearly be seen as changing the DoA at the distance of 30 m in Fig. 6(b). The difference

between the “best” and the “worst” cases in studying the effects of azimuth orientation on capacity is significant [see Fig. 9(a)]. The use of copolarized or dual-polarized elements (case 2) does not significantly affect the capacity result—two polarizations being slightly better. Increasing the interelement spacing of FS elements (case 3) does not provide so much increase in capacity as in an outdoor environment since the indoor environment is more scatter rich. However, the increase is about 1 bits/s/Hz as the distance changes from  $0.7\lambda$  to  $3.5\lambda$ .

The capacities of all the studied dipole arrays are of almost equal size [Fig. 9(d), case 4]. Using two polarizations provides the best capacity—a solution which is, however, only slightly better than using four vertical dipoles. Generally speaking, the average capacity of dipole configurations is approximately 2 bits/s/Hz lower than that of the corresponding directive patch antenna configuration because the patches have larger element gain than the dipoles. The variance of the capacity of the patch configurations is clearly higher than that of the dipoles due to the significant effect of azimuth orientation of the patch array



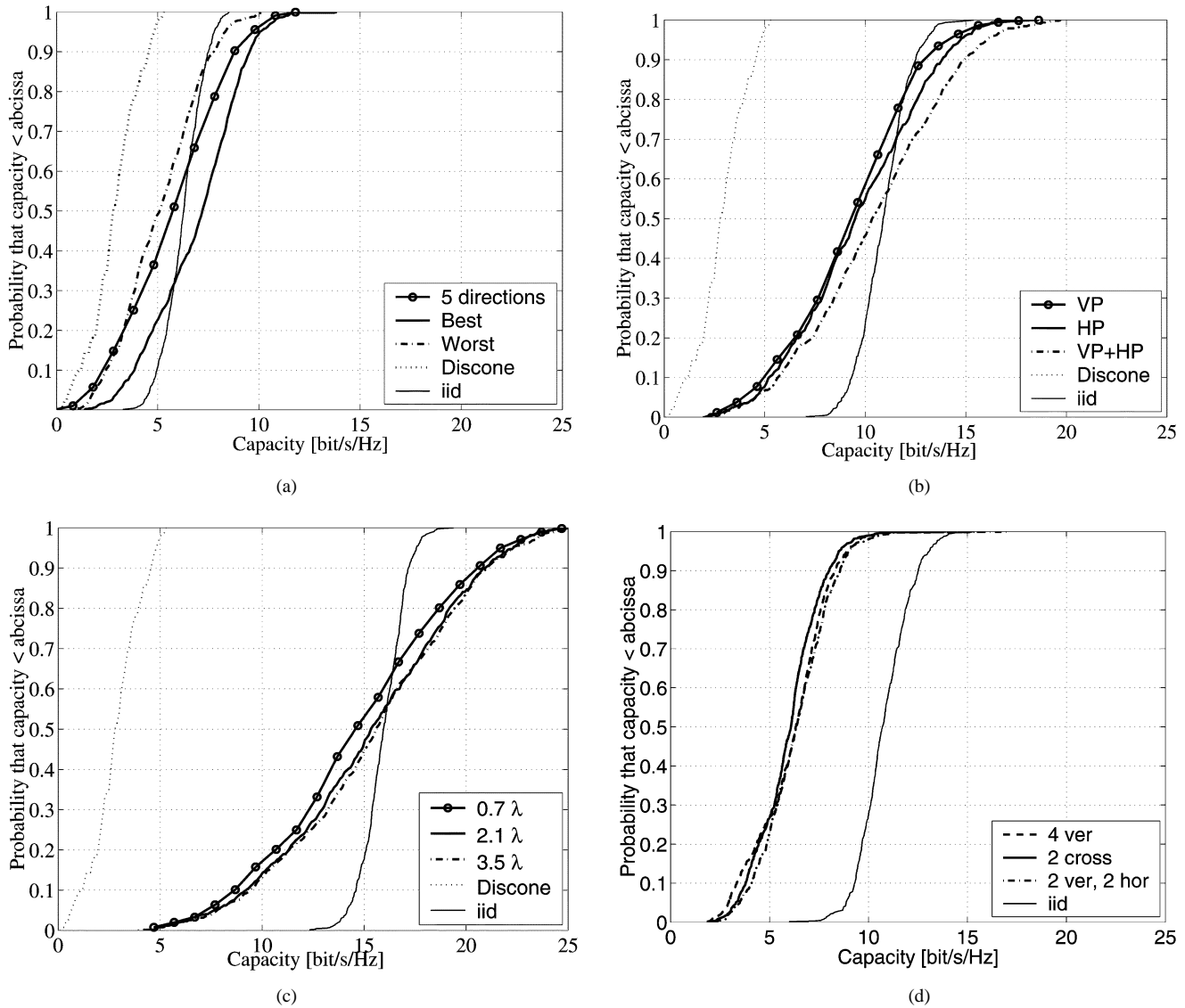


Fig. 10. Capacity results in the indoor environment FS1 “B.” (a) Case 1, the effect of azimuth orientation,  $n_T = 4$ ,  $n_R = 2$ . (b) Case 2, the effect of polarization,  $n_T = 4$ ,  $n_R = 4$ . (c) Case 3, the effect of Tx element spacing,  $n_T = 4$ ,  $n_R = 8$ . (d) Case 4, the dipole study,  $n_T = 4$ ,  $n_R = 4$ .

on the capacity, as well as variations in MIMO gain along the measurement route.

### C. Indoor Route “B” FS Location 1

The route “B” begins in an open hall and ends in a lecture room. In Fig. 6(c), a  $90^\circ$  turn at a distance of 6 m in the middle of the route can be seen as a change in the DoA. In this environment, the capacity varies 2.5 bits/s/Hz according to the azimuth orientation of the MS [Fig. 10(a)], which is less than in the two other environments. Orthogonal polarizations and directive elements increase the capacity by approximately 1 bit/s/Hz compared with that of copolarized elements (case 2). Increasing the distance between elements at the FS (case 3) does not increase the capacity as in the outdoor environment. The average capacity of dipole arrays is approximately 3 bits/s/Hz lower than the corresponding capacity of the dual-polarized patch antennas in case 2. Differences between three dipole antenna arrays are almost negligible (case 4) although a larger difference between

the copolarized and orthogonally polarized dipole configurations was expected.

### D. Number of Elements at FS

The MIMO system is based on several subchannels transferring data simultaneously at the same bandwidth. The effects of increasing the number of Tx elements on the average capacity for real antenna configurations and corresponding i.i.d. are presented in Fig. 11. The adjacent elements (1 element = 2 channels) were added gradually from one to seven. At the MS, configurations of the four dual-polarized elements were analyzed in five azimuth angles.

In all the environments studied, capacity increases most as the number of Tx elements increases from one to four – corresponding to an increase of between two and eight in the number of possible eigenvalues. The spread of eigenvalues also increases with the number of antennas. Since four elements were used at the MS, the maximum number of eigenvalues is

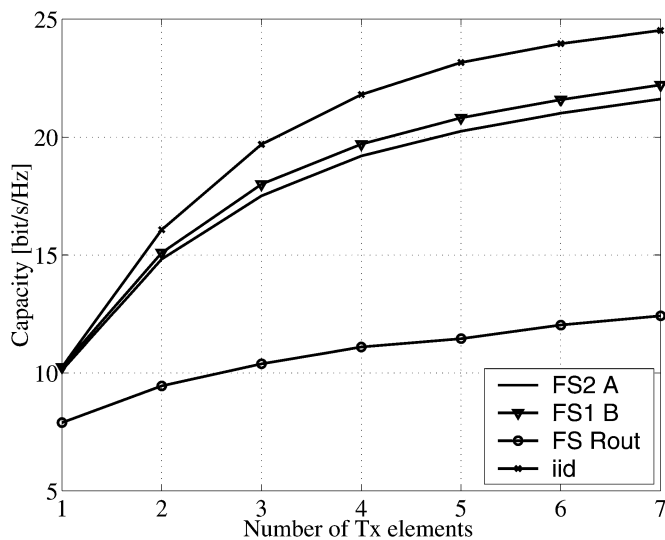


Fig. 11. Capacity as a function of number of FS antenna elements in different environments. The number of elements has been four at the MS.

eight. However, as more than four elements are used at the FS, the capacity increases further because of the increased antenna array gain. In the urban environment, the effect of the number of elements on capacity seems to be of lesser importance than that of the indoor environment. Although the same antenna arrays are used, the resultant difference between the outdoor and indoor environments is surprisingly large—approximately 8 bits/s/Hz—due mainly to different conditions of propagation.

## V. CONCLUSION

Several realistic antenna configurations were studied using two methods: either selecting elements from the antenna arrays used in measurements or using the incident field-based analysis. A useful methodological issue was discovered to be the use of an omnidirectional “pilot” antenna for normalization, which enables us to avoid the automatic increase of the transmitted power when a directive antenna points in a low-incident power direction, as toward a wall. This method, thus, brings the evaluation of mobile antennas closer to the widely accepted mean effective gain analysis used for SISO systems [18]. The combination of the analysis of incident waves and the achieved capacity was found to be a very convenient when explaining capacity results.

In increasing the capacity, the use of orthogonally polarized Rx elements was found to be equally effective with the copolarized elements: the former being 14% better. This supports the utilization of compact dual-polarized antennas in the mobile terminal.

In comparison with the capacity of a standard SISO configuration it seemed obvious that the large scale fluctuation of the achieved MIMO capacity is larger with directive antenna configurations than with omnidirectional. Moreover, for the larger MIMO antenna configurations, not only the average capacity, but also the fluctuation of the capacity increases due to the spread distribution of eigenvalues. This means that the effective “slow fading” in the MIMO radio systems depends on the antenna configuration—a fact that should also be taken into ac-

count in network planning, in addition to the average increasing of the capacity.

Increasing the distance between elements at the FS increases capacity, especially in the urban outdoor environment where signals arrive at the MS from certain azimuth directions. In a street canyon-type outdoor environment, more diversity is obtained by increasing the element spacing; thus resulting in an increased MIMO capacity of 33% between distances of  $0.5\lambda$  to  $2.5\lambda$ . Due to a larger angular spread, the element spacing has only an effect of 7% on the indoor capacity. The distance between the antenna elements at the FS is not so important in our measurements as it was in [11] since we used directive elements and two orthogonal polarizations with lower correlation between the elements, compared with, for example, omnidirectional dipoles. At the MS, directive elements result in 35% higher average capacities than those of the omnidirectional elements.

The number of elements of the FS is important indoors but less significant outdoors. An indoor environment is more scatter-rich and signals propagating along different paths can be utilized more effectively by adding more antenna elements. The capacities achieved indoors are surprisingly much, 70% higher than outdoors. This is obviously due to the increased number of parallel paths, so there is an actual MIMO gain. Outdoors, in street canyons, the increase in capacity is more a result of increased effective antenna gain, since the angular spread is nevertheless narrow.

## ACKNOWLEDGMENT

The authors would like to thank M. Toikka for help with measurements.

## REFERENCES

- [1] R. G. Vaughan and J. B. Andersen, “Antenna diversity in mobile communications,” *IEEE Trans. Veh. Technol.*, vol. 36, pp. 149–172, Nov. 1987.
- [2] G. J. Foschini, “Layered space-time architecture for wireless communication in a fading environment when using multi-element antennas,” *AT&T Bell Labs. Tech. J.*, pp. 41–59, 1996.
- [3] D.-S. Shiu, G. J. Foschini, M. J. Gans, and J. M. Lahn, “Fading correlation and its effect on the capacity of multielement antenna systems,” *IEEE Trans. Commun.*, vol. 48, pp. 502–513, Mar. 2000.
- [4] G. J. Foschini and M. J. Gans, “On limits of wireless communications in a fading environment when using multiple antennas,” *Wireless Pers. Commun.*, vol. 6, pp. 311–335, 1998.
- [5] J. B. Andersen, “Antenna arrays in mobile communications: Gain, diversity, and channel capacity,” *IEEE Antennas Propagat. Mag.*, vol. 42, pp. 12–16, Apr. 2000.
- [6] C. C. Martin, J. H. Winters, and N. R. Sollenberger, “MIMO radio channel measurements: Performance comparison of antenna configurations,” in *Proc. IEEE 54th Vehicular Technology Conf.*, vol. 2, 2001, pp. 1225–1229.
- [7] D. Chizhik, G. J. Foschini, and R. A. Venezuela, “Capacities of multi-element transmit and receive antennas: Correlation and keyholes,” *Electron. Lett.*, vol. 36, pp. 1099–1100, June 2000.
- [8] R. G. Gallager, *Information Theory and Reliable Communication*. New York: Addison-Wesley, 1968.
- [9] M. Steinbauer, A. F. Molish, and E. Bonek, “The double-directional radio channel,” *IEEE Antennas Propagat. Mag.*, vol. 43, pp. 51–63, Aug. 2001.
- [10] R. S. Thomä, D. Hampicke, A. Richter, and G. Sommerkorn, “Measurement and identification of mobile radio propagation channels,” in *Proc. IEEE Instrumentation and Measurement Conf.*, vol. 3, 2001, pp. 354–357.

- [11] D. Chizhik, F. Rashid-Farrokhi, J. Ling, and A. Lozano, "Affect of antenna separation on the capacity of BLAST in correlated channels," *IEEE Commun. Lett.*, vol. 4, pp. 337–339, Nov. 2000.
- [12] J. P. Kermaol, L. Schumacher, F. Fredriksen, and P. E. Mogensen, "Polarization diversity in MIMO radio channels: Experimental validation of a stochastic model and performance assessment," in *Proc. IEEE 54th Vehicular Technology Conf.*, vol. 1, 2001, pp. 22–26.
- [13] J. P. Kermaol, P. E. Mogensen, S. H. Jensen, J. B. Andersen, F. Fredriksen, T. B. Sorensen, and K. I. Pedersen, "Experimental investigation of multipath richness for multi-element transmit and receive antenna arrays," in *Proc. IEEE 51th Vehicular Technology Conf.*, vol. 3, 2000, pp. 2004–2008.
- [14] C. C. Martin, J. H. Winters, and N. R. Sollenberger, "Multiple input multiple-output (MIMO) radio channel measurements," in *Proc. IEEE 52th Vehicular Technology Conf.*, vol. 2, 2000, pp. 774–779.
- [15] J. Kivinen, P. Suvikunnas, D. Perez, C. Herrero, K. Kalliola, and P. Vainikainen, "Characterization system for MIMO channels," in *Proc. 4th Int. Symp. Wireless Personal Multimedia Communications*, Sept. 2001, pp. 159–162.
- [16] K. Kalliola, H. Laitinen, L. Vaskelainen, and P. Vainikainen, "Real-time 3-d spatial-temporal dual-polarized measurement of wideband radio channel at mobile channel," *IEEE Trans. Instrum. Meas.*, vol. 49, pp. 439–446, Apr. 2000.
- [17] J. Kivinen, T. Korhonen, P. Aikio, R. Gruber, P. Vainikainen, and S.-G. Häggman, "Wideband radio channel measurement system at 2 GHz," *IEEE Trans. Instrum. Meas.*, vol. 48, pp. 39–44, Feb. 1999.
- [18] K. Kalliola, K. Sulonen, H. Laitinen, O. Kivekäs, J. Krogerus, and P. Vainikainen, "Angular power distribution and mean effective gain of mobile antenna in different propagation environments," *IEEE Trans. Veh. Technol.*, vol. 51, pp. 823–838, Sept. 2002.
- [19] C. A. Balanis, *Antenna Theory: Analysis and Design*. New York: Wiley, 1997, pp. 133–164.
- [20] N. Amitay, M. J. Gans, H. Xu, and R. A. Valenzuela, "Effects of thermal noise on accuracy of measured blast capacities," *Electron. Lett.*, vol. 37, pp. 591–592, 2001.
- [21] M. J. Gans, N. Amitay, Y. S. Yeh, X. Hao, T. C. Damen, R. A. Valenzuela, T. Sizer, R. Storz, D. Taylor, W. M. MacDonald, and T. C. A. Adamiecki, "Outdoor BLAST measurement system at 2.44 Ghz: Calibration and initial results," *IEEE J. Select. Areas Commun.*, vol. 20, pp. 570–583, Apr. 2002.
- [22] K. Kalliola, H. Laitinen, K. Sulonen, L. Vuokko, and P. Vainikainen, "Directional radio channel measurements at mobile station in different radio environments at 2.15 Ghz," in *Proc. 4th Euro. Personal Mobile Communications Conf.*, Feb. 2001.



**Kati Sulonen** was born in Helsinki, Finland, in 1973. She received the M.Sc. and the Licentiate of Science degrees in technology from Helsinki University of Technology (HUT), Espoo, Finland, in 1999 and 2001, respectively. She is currently working toward the Ph.D. degree in technology at HUT.

From 1995 to 1998, she was with Siemens Finland. From 1998 to 1999, she worked at the Radio Laboratory, HUT, as a Research Assistant. Since 1999, she has been there as a Researcher. Her current research

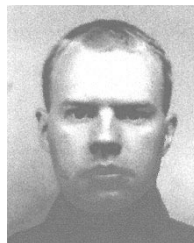
interests are in the evaluation of performance of mobile terminal antennas.



**Pasi Suvikunnas** was born in Tuusula, Finland, in 1967. He received the B.Sc. degree in technology from Technical Institute of Helsinki, Helsinki, Finland, in 1994, and the M.Sc. and Licentiate of Science degrees in technology from Helsinki University of Technology (HUT), Espoo, Finland, in 1999, and 2002, respectively. He is currently working toward Ph.D. degree in technology.

Since 1999, he has been with the Radio Laboratory, HUT, as a Researcher. His current fields of interest are multielement antennas and mobile radio

propagation.



**Lasse Vuokko** was born in Vantaa, Finland, in 1977. He received the M.Sc. degree in technology from Helsinki University of Technology (HUT), Espoo, Finland, in 2001.

Since 1999, he has been with the Radio Laboratory, HUT, first as a Research Assistant and later as a Researcher. His current research interests include mobile radio propagation and radio channel measurements.



**Jarmo Kivinen** was born in Helsinki, Finland, in 1965. He received the degree of M.Sc., Licentiate of Science, and the Ph.D. degrees in technology from Helsinki University of Technology (HUT), Espoo, Finland, in 1994, 1997, and 2001, respectively, in electrical engineering.

Since 1994, he has worked as a Research Engineer and Project Leader at Radio Laboratory, HUT, and from 1995 to 1996 as an RF Design Engineer at Nokia Telecommunications, Espoo, Finland. His main fields of interest are multidimensional radio propagation channel measurement and modeling techniques, and RF techniques in radio communications.



**Pertti Vainikainen** (M'91) was born in Helsinki, Finland in 1957. He received the M.Sc., Licentiate of Science, and the Ph.D. degrees in technology from Helsinki University of Technology (HUT), Espoo, Finland, in 1982, 1989, and 1991, respectively.

He was Acting Professor of radio engineering from 1992 to 1993, Associate Professor of radio engineering since 1993, and Professor in radio engineering since 1998, all at the Radio Laboratory, HUT. From 1993 to 1997, he was the Director of the Institute of Radio Communications (IRC), HUT and a Visiting Professor at Aalborg University, Denmark, in 2000. His main fields of interest are antennas and propagation in radio communications and industrial measurement applications of radio waves. He is the author or coauthor of three books and about 140 refereed international journal or conference publications and the holder of four patents.